Ročník 2011 electroscope Číslo II

# Artificial defects of solar cells

P. Škarvada, P. Tománek, T. Palai-Dany
Department of Physics, Faculty of Electrical Engineering and Communication, Brno University of Technology, Technická 8, Brno
E-mail: xskarv03@stud.feec.vutbr.cz

**Abstract**:
Artificial defects of solar cells are observable with laser beam induced current techniques. Reversed bias solar cell light emission can also reveal structure inhomogenity and local mechanical damage of the sample. The paper shows simple method for basic classification into structure group and artificial defects group. Observed artificial defects are shown and process of its creation is described. Defects classification method is based on the measurement of light emission at fixed reverse voltage while the temperature of sample is changing in the range of 20 K. There is different light emission temperature dependence in the case of bulk defects and mechanical damage defects. Experimental light emission data are consequently correlated with laser beam induced current map.

## INTRODUCTION

During fabrication process of solar cell some structure imperfection can arise. Electrical measurement of solar cells is being widely used for the quality control and solar cell inspection purpose. Although electrical measurements can reveal defects and certain sample properties, for the defect localization and its classification, other techniques have to been used. The most widespread methods are based on photoelectrical measurements allowing determine local cell performance and localize defective areas. Nevertheless, for determination of particular defect nature advanced microscopic and structural techniques are necessary.
Defects or imperfections are substructures in solar cell structure that can lead to the destruction of solar cell under certain operation conditions. They can also be responsible for the deterioration of the solar cell parameters. Information about serious defects is important for modification of fabrication process to avoid or suppress them.
The testing has to be clearly defined, repeatable with well known uncertainty, and should not affect investigated sample parameters. In this case the testing is called nondestructive testing. Of course, from the production point of view, the testing should be also fast enough.
Except optical study, photoluminescence techniques and electromagnetic testing, the absolute majority of testing methods require samples wired into measurement circuit or excitation circuit. Especially in laboratory conditions the connecting differs with each sample and experiment. Now a thickness of ordinary monocrystalline solar cell is only of several hundreds of micrometers, hence the clutch connecting can generate local cracks. Therefore a special effort is claimed for proper and nondestructive electrical connecting of samples.

## METHOD

### Laser beam induced current

Laser beam induced current (LBIC) is a method generally used for defect localization in structure of exposed pn junction. The method is based on interaction of laser beam with matter [1]. Focused incident photons generate carriers in optically excited pn junction area. This local current response is then measured. By scanning of laser beam the LBIC image can be acquired.
The current can be measured as a voltage drops at sufficiently low resistance, but preferable is measured using transimpedance amplifier TIA due to zero input impedance. TIA has a high gain and together with input capacity the phase margin is decreasing. So TIA usually inclines to the oscillation. Especially for solar cell, which has relatively high capacity compared to small photodiode, proper feedback capacitor has to be used to restore phase margin [2].

### Light emission from biased sample

The light emission can occur in both direct and indirect semiconductors when they are electrically biased. Moreover emission of photons can also occur in imperfection regions while the sample is under reverse biased conditions [3, 4].
For an injection process the sample is biased in forward direction and the emission peak corresponds to the energy gap of junction. Although indirect semiconductors are considered as bad electroluminescence sources, electroluminescence can also be measured there. In this case, electroluminescence can be used for detection of cracks, mapping of series resistances as well as of minority carrier diffusion length distribution.
On the other side, the apparition of light emission from reverse biased solar cell is also very interesting effect. Generally a photon emission can only occur

during photon exchange process. Shockley-Read-Hall and Auger recombination are considered as non-radiative processes. In reverse bias condition, the recombination of electron-hole pair can happen via avalanche multiplication, carrier tunneling and incandescence in the case of resistive defects.
Sensitive measurement system with photon counting PC cooled photomultiplier tube (PMT) has been employed for the detection of weak light emission (Fig.1). A sample of solar cell was placed in thermally stabilized electrode system and the bias was controlled by computer. The scanning probe collects light emission over the sample. PMT was used as detector in PC mode [5]. The PMT has been mainly working in visible range where the peak sensitivity was located (wavelength range from 350 to 800 nm).

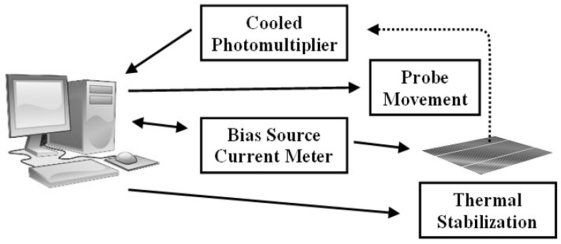


Fig. 1: Computer controlled measurement system for low radiant flux detection using photon counting mode

As it was shown in [6], there are several types of solar cell defects caused by cracks and holes, inclusions, precipitates, etc.

### Thermal properties of light emission

Nevertheless, some defects are observed in current voltage characteristics like a partial breakdown. Thermal dependence of this breakdown was correlated with thermal dependence of light emission as was reported in [7]. Moreover thermal dependence of light emission from bulk and edge imperfections shows different characteristics, respectively. Hence not all of the light emitting spots have the same nature. In some cases, they could be connected with avalanche multiplication or microplasmas, but the further study of this problem is foreseen in our laboratory.

## EXPERIMENTAL

### Laser beam induced current (LBIC)

Selected part of solar cell sample α (Fig. 2) and whole sample β (Fig. 3) were tested with LBIC method.
In Fig. 2 the border of solar cell sample α can be seen on the top of the image. Black horizontal lines are top sample contacts. These parts of solar cell do not contribute to integral solar cell current. Interesting cross can be seen in the lower right part of the image.

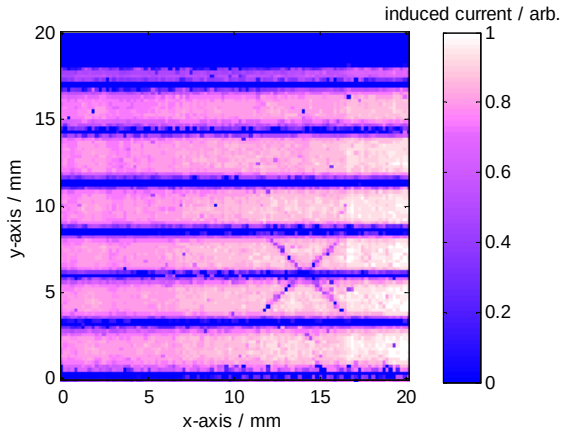


Fig. 2: Laser beam induced current map of selected solar cell sample α ($T$ = 298 K)

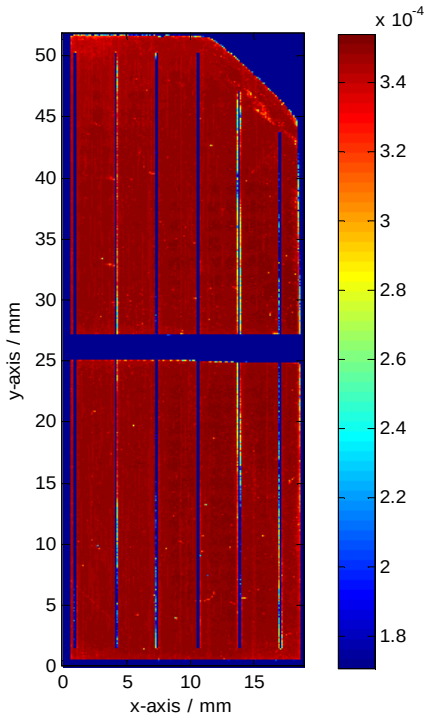


Fig. 3: Laser beam induced current map of selected solar cell sample β ($T$ = 300 K), color map correspond to short circuit current

This cross is not visible with ordinary optical microscope. Nevertheless this cross is a microcrack in the crystal turned in crystal lattice directions. This crack was created by connecting the sample for electrical measurement. Too heavy connecting probe force leads to creation of this crack. Although sample sticks together small stress will break the sample into several pieces.
LBIC map of the second selected sample β is shown in Fig. 3. Some local damage close to the thin top contacts can be seen. These small scratches were created during multiple electrical connection of the sample with testing devices. For connection of the top side of the sample, an improper probe and too high adherence force were used. This led to sliding of probe outside the contact and damage of solar cell surface structure.

### Light emission from biased sample

The same area of sample α (Fig. 2) was consequently tested for light emission under reverse bias. The reverse bias of solar cell was increased while the reverse current has been set bellow 13.0 mA. This is the safe current density value for given sample that does not cause the sample degradation. While using this criterion the reverse voltage of $U_R$ = 24.0 V was reached. After that, the light emission was measured over the sample surface. Resulting light emission map is in Fig. 4. Here, the color map matches the logarithm of detected counts per second.

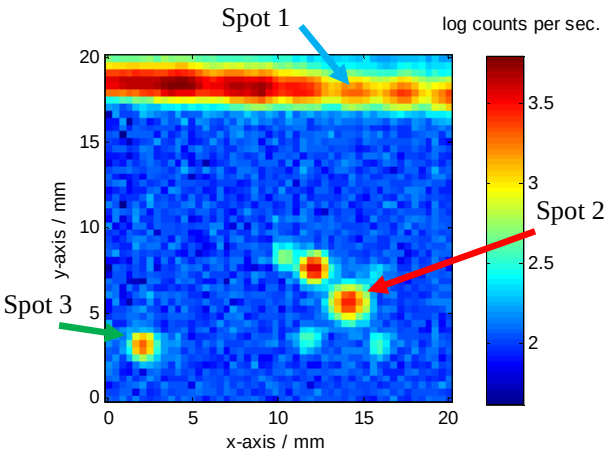


Fig. 4: Light emission from reverse biased sample α ($U_R$ = 24.0 V, $T$ = 298 K)

The phenomena of visible light emission from border can be seen. In this lighting border one of the luminous spots "spot 1" has been selected for further testing. In the bulk area, there are several localized light emitting spots. Note, that in area of LBIC cross (Fig.2), the light emission in visible range occurs and has the same shape as in LBIC case. This means that this light emission is a consequence of crystal microcrack made by sample testing. Main spot of this part was then selected for further testing as "spot 2". The last light emitting spot is marked "spot 3". There is no correlation with LBIC map in the case of the spot 3.

The sample β was also tested under reverse bias. As result, a light emission at reverse voltage $U_R$ = 22.0 V can be seen in Fig. 5. In the left side there is light emission before local damage by repetitive electrical connection on the top side contacts. Sample was repeatedly connected in green circles area (17 points). In the right part of Fig. 5, there is the same sample after described connection procedure. The new nine lighting spots arise in areas of probe connection. In this case, there is also a proof that mechanical surface damage can lead to light emission from sample under reverse bias. Four spots A, B, C, D were selected here for the further testing. Two spots were presented on the sample before probe connection and two were made mechanically after that.

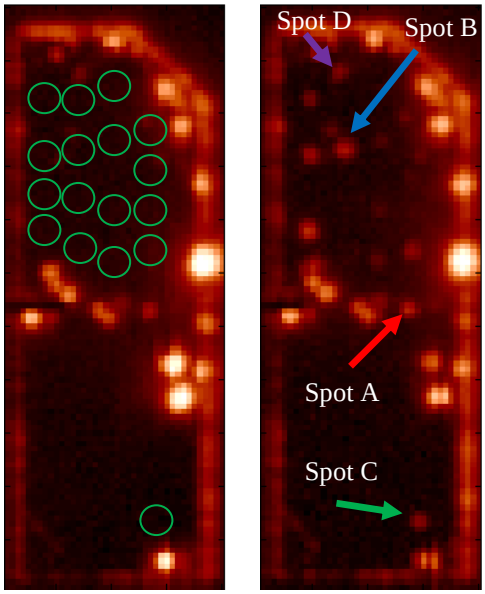


Fig. 5: Light emission from reverse biased sample β ($U_R$ = 22.0 V, $T$ = 300 K)

### Thermal properties of light emission

Light emission vs. sample temperature has been measured for three selected spots of sample α. Solar cell sample was biased from voltage source $U_R$ = 24 V during the measurement. Light emission from spots 1 and 2 reflects a positive thermal dependence, while a negative thermal dependence from bulk spot 3 has been observed (Fig. 6).

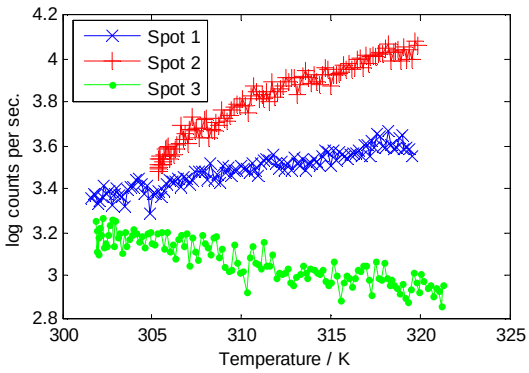


Fig. 6: Thermal properties of light emission of selected spots in sample α ($U_R$ = 24 V)

Light emission vs. sample temperature has also been measured for four selected spots of sample β. For avalanche type breakdown, the negative light emission temperature relation is expected. With growing temperature the crystal lattice vibration increases and hence the carrier movement is inhibited. Consequently a breakdown voltage increases with temperature, and light emission is decreasing. This result means that only a "spot 3" is caused by avalanche multiplication. Although all bulk spots have negative thermal dependence, they are not all due to the avalanche breakdown. Each

contamination can also lead to the light emission [8]. Exact explication of all defects is not fully clear yet.
Solar cell sample was biased from voltage source $U_R = 22$ V during the measurement. Light emission from spots A and D reflects a negative thermal dependence, while spots B and C have positive thermal dependence (Fig. 7) [9]. Since the light emissions from selected spots have considerably different value, measurement curves were normalized to fit one plot. Note that spots A and D were presented on the sample before local mechanical damage whilst spots B and C are artificial defects.

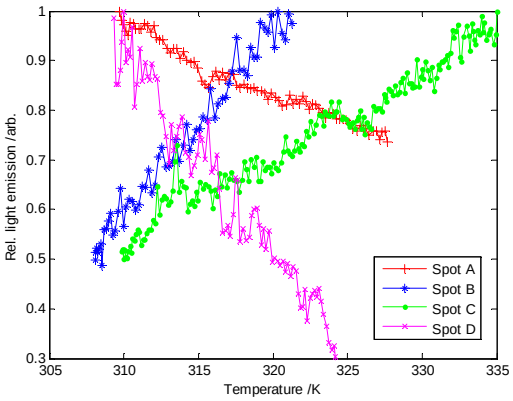


Fig. 7: Thermal properties of light emission of selected spots in sample β ($U_R = 22$ V)

However for positive light emission temperature dependence, Zener and thermal breakdowns come into question. Zener breakdown is highly improbably due to breakdown voltage and sample carrier concentration.
Defects which are caused by microstructure snapping, surface scratching and border defects have the same (positive) thermal dependence. All other tested bulk defects (more than hundred tested defects) have negative light emission thermal dependence.
If the light emission of one defect versus reverse bias voltage is plotted, one can find out that this plot has nonlinear character. Therefore the slope of curves in Fig. 6 and Fig. 7 are incomparable and strongly depend on reverse bias. From the measurement, only a slope sign is valuable.

**Microscale study of bulk defect**

The area of sample α (around a spot 3) was measured using scanning probe microscope to visualize the imperfection surface in micro-scale (Fig.8). One can observe, and resolve, unique structures (probably inclusions) providing local change of electric field distribution. Hence the breakdown will occur in this sample area when the sample is biased enough. Scanning near-field optical microscope can be used for the light detection with so called "superresolution" [10]. Light emission comes out from small area near the center of the image.

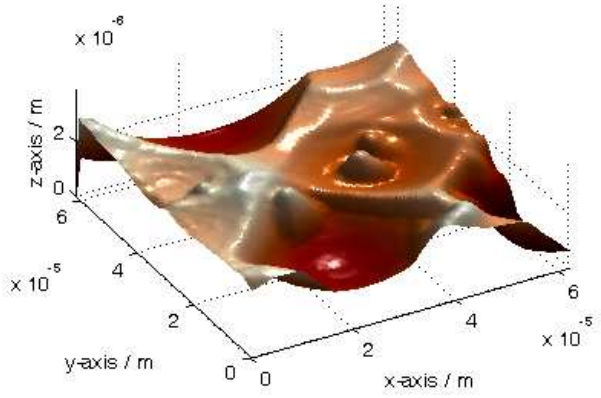


Fig. 8: Microscopic image of the sample surface (spot 3)

## CONCLUSIONS

It has been demonstrated that light emission from reverse biased solar cell can reveal structure inhomogenities. Together with control of sample temperature this method provides a basic defect classification. We have discovered, that only 20 K temperature range is enough for this classification.
During a connection of sample, two types of defect can arise. The first one is a crystal crack caused by too heavy force of connecting probe. The second one is snapping of microstructure caused by scratch of sharp probe over the sample surface.
Bulk structure defects show negative light emission temperature dependence while the border emission, microstructure cracks and snapping defects show positive light emission temperature dependence.
Crack defects were revealed using LBIC measurement. There is evident correlation there between LBIC image and light emission image taken in the same sample area at $U_R = 24$ V. The bulk spot 3 which has different thermal dependence than other two investigated spots, was measured by scanning probe microscopy. Unique structures in the surface were observed, that are probably the inclusions. They provide local changes of electric field distribution and can lead, under some bias conditions, to the local breakdown.

## ACKNOWLEDGEMENT

This research has been supported by the Grant Agency of the Czech Republic within the framework of the project GA P102/10/2013, and by the Czech Ministry of Education in the frame of MSM 0021630503 Research Intention MIKROSYN "New Trends in Microelectronic System and Nanotechnologies", as well as by grant Kontakt LH11060. These supports were gratefully acknowledged.

## REFERENCES


[1] M. Allmen and A. Blatter, Laser-beam interactions with materials: Physical principles and applications, Heidelberg, Springer, 1995.

[2] J. G. Graeme, Photodiode amplifier, Op Amp solutions, New York, McGraw-Hill, 1996.

[3] R. Newman, “Visible light from a silicon p-n junction”. Phys. Rev., vol. 100, pp. 700-703, 1955.

[4] P. Tománek, et al. “Local investigation of monocrystalline silicon solar cells defects”, in 37th IEEE PVSC conference, Seattle, USA, 2011 (submitted)

[5] P. Škarvada, et al.“ Microscale localization of low light emitting spots in reversed-biased silicon solar cells”, Sol. Energ. Mat. Sol. C., vol. 94, pp. 2358-2361, 2010.

[6] O. Breitenstein, et al., “Shunt types in crystalline silicon solar cells”. Prog. Photovolt: Res. Appl, vol. 12, pp. 529-538, 2004.

[7] P. Škarvada and P. Tománek, “Reverse-biased solar cell light emission thermal dependence” in Electronic Devices and Systems EDS10, Brno, pp. 304-307, Novpress, 2010.

[8] O. Breitenstein, et al., “Understanding junction breakdown in multicrystalline solar cells”. J. App. Phys., vol. 109, 2011.

[9] L. Grmela et al., Near-field detection and localization of defects in monocrystalline silicon solar cell, Inventi Rapid: Energy and Power, vol. 2011, pp.61-64, 2011

[10] M. J. Romero, “Novel applications of near-field scanning optical microscopy: microlumin-escence from local junction breakdown in solar cells” in Photovoltaic Specialist Conference 2010, Honolulu, pp. 219-223, 2010.